



Cite this: *Med. Chem. Commun.*,  
2015, 6, 1370

Received 30th April 2015,  
Accepted 12th June 2015

DOI: 10.1039/c5md00189g

www.rsc.org/medchemcomm

## Enhanced *in vitro* and *in vivo* uptake of a hydrophobic model drug coumarin-6 in the presence of cucurbit[7]uril†‡

Xiaoqing Miao,<sup>a</sup> Ye Li,<sup>a</sup> Ian Wyman,<sup>b</sup> Simon M. Y. Lee,<sup>a</sup> Donal H. Macartney,<sup>b</sup>  
Ying Zheng<sup>\*a</sup> and Ruibing Wang<sup>\*a</sup>

This report describes, for the first time, cucurbit[7]uril-assisted quantitative *in vitro* and *in vivo* uptake of a hydrophobic model drug, coumarin-6, by both an epithelial cell model and a zebrafish model. The transcellular delivery pathway study suggested multiple mechanisms involved, including macropinocytosis, clathrin and lipid raft-mediated endocytosis/exocytosis.

High-throughput screening approaches in drug discovery and development have led to an increasing number of lipophilic drugs whose clinical usefulness is often hampered by their poor solubility in water, as water-solubility is one of the main factors to influence drug bioavailability.<sup>1,2</sup> One of the popular approaches to improve the water solubility and bioavailability of drug candidates is to encapsulate them within macrocyclic molecular containers such as cyclodextrins, calixarenes, and cucurbiturils.<sup>3–6</sup> In particular, cyclodextrins have been studied for over 100 years and frequently used in pharmaceutical sciences to enhance the aqueous solubility of drugs and to improve drug bioavailability, *e.g.*, several dozens of commercial pharmaceutical products based on cyclodextrins have been approved by regulatory agencies.<sup>3,7</sup> Accordingly, the cellular uptake of both cyclodextrins and calixarenes, as well as the associated mechanisms, have been extensively studied.<sup>8,9</sup> The cucurbit[*n*]urils (CB[*n*], *n* = 5–8, 10, 14), are a relatively new family of macrocyclic host molecules that have received increasing attention during the past 15 years. Consequently, investigations into their potential applications in the pharmaceutical sciences such as drug formulation and delivery are still far from real-world clinical use, presumably due to the scarcity of examples exhibiting both *in vitro* and *in vivo* uptake of a hydrophobic drug promoted by CB[*n*] and the lack of understanding of the associated transcellular mechanisms involved with CB[*n*]-drug complexes.<sup>5,6,10</sup>

Recently CB[*n*] hosts have demonstrated outstanding molecular recognition properties and superior interactions with a wide range of neutral and positively charged molecules, many of which are biologically- and medically-relevant compounds.<sup>5,6,11</sup> Among the CB[*n*] family, CB[7] (shown in Fig. 1) has received perhaps the greatest attention as a potential drug delivery vehicle due to its well-studied biocompatibility profile,<sup>12–15</sup> superior water-solubility and compatible size with various organic and organometallic drug molecules.<sup>5,6,11</sup> Examples of drugs that have been studied by us and by a few other research groups for their complexation behaviour with CB[7] include: a beta-blocker atenolol,<sup>16</sup> a tuberculosis drug pyrazinamide,<sup>17</sup> platinum-based anti-cancer drugs such as cisplatin and several others,<sup>18,19</sup> local anesthetics,<sup>20</sup> an anticoagulant drug coumarin,<sup>21</sup> an anti-peptic ulcer drug ranitidine,<sup>22</sup> and vitamin B<sub>12</sub> as well as coenzyme B<sub>12</sub>.<sup>23</sup> Although these and other examples have exhibited enhanced water solubility as guest drugs upon CB[7] encapsulation, the actual benefit of such encapsulation during drug delivery (*e.g.* increased drug uptake), has not been clearly demonstrated with both *in vitro* and *in vivo* models. One previous study has reported the cellular uptake of CB[7] complexed acridine orange and pyronine by a mouse muscle embryo 3T3 cell model *via* fluorescence microscopy.<sup>24</sup> Another study showed the uptake and trafficking of fluorescent dye tagged CB[7] with macrophage cell lines RAW264.7 by using flow cytometry and fluorescence microscopy.<sup>25</sup> However, the cellular uptake of these complexes was not

<sup>a</sup> State Key Laboratory of Quality Research in Chinese Medicine, Institute of Chinese Medical Sciences, University of Macau, Taipa, Macao, China.

E-mail: yzheng@umac.mo, rwang@umac.mo; Tel: +853 8822 4689, +853 8822 4687

<sup>b</sup> Department of Chemistry, Queen's University, Kingston, ON, K7L 3N6, Canada

† The financial support of this research by University of Macau and NSERC-Canada is gratefully acknowledged.

‡ Electronic supplementary information (ESI) available. See DOI: 10.1039/c5md00189g

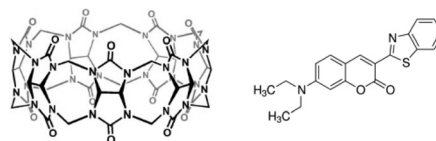


Fig. 1 The molecular structures of CB[7] (left) and C6 (right).



compared with free guests (which can also cross cell membranes by themselves in both of these cases) in these studies. Thus the value of CB[7] as a delivery vehicle for the guest drug was not exhibited. One recent study demonstrated that CB[7] aided the transportation of a synthetic hemicyanine dye (Hsd) into living cells, thus facilitating selective RNA staining.<sup>26</sup> However, the intracellular transportation mechanism of these complexes has never been studied previously.

Herein we report the CB[7]-assisted cellular uptake of a hydrophobic model drug and a fluorescent dye, coumarin-6 (C6, Fig. 1), by a Madin-Darby canine kidney (MDCK) epithelial cell model. The MDCK cell line is a widely adopted epithelial model that is used to simulate biological barriers such as the gastrointestinal tract and blood brain barriers, and these barriers are often the main hindrance against the uptake of various substances *in vivo*, including new chemical entities and therapeutic agents.<sup>27</sup> Thus it is critical to understand whether CB[7] can assist the endocytosis and exocytosis of encapsulated hydrophobic drugs with this epithelial cell model. In this communication, the benefits of CB[7] in the cellular uptake of a hydrophobic model guest drug by this important barrier tissue cell model was demonstrated for the first time. Importantly, it was found that CB[7] significantly improved the cellular uptake of the model drug. The trans-cellular transportation mechanism has also been studied in detail. Furthermore, the enhanced model drug uptake was further examined with a live *in vivo* zebrafish model.

C6 is a derivative of coumarin in the benzopyrone chemical class. It is a natural substance found in many plants, often used as a fluorescent and lipophilic model drug for the *in vitro* or *in vivo* monitoring of nanoparticle-based delivery systems *via* fluorescence microscopy.<sup>28</sup> As a highly lipophilic model drug, it is not readily taken up by MDCK cells.<sup>27</sup> As a matter of fact, the formation of a 1:1 guest-host complex between C6 and CB[7] at neutral pH has been previously confirmed by <sup>1</sup>H NMR spectroscopy as well as UV-visible absorbance (Job's plot) and emission spectroscopy (titration), with a binding constant of  $(2.0 \pm 0.1) \times 10^3 \text{ M}^{-1}$ .<sup>29</sup> A MM2 energy-minimized structure of the C6@CB[7] complex (Fig. 2) shows that the benzopyrone portion is encapsulated within the CB[7] cavity, aligning the quaternary amine (protonated at neutral pH) at one of its portals and leaving the benzothiazole ring outside of cavity. Such an encapsulation configuration is consistent with our previous

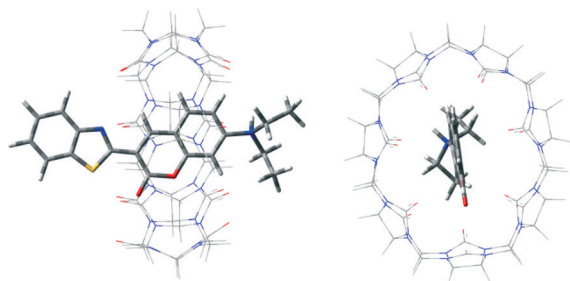


Fig. 2 Molecular modeling of C6@CB[7] (side view and top view).

results from investigations focusing on the encapsulation of the parent coumarin by CB[7].<sup>21</sup>

Prior to the *in vitro* and *in vivo* delivery study, the biocompatibility of CB[7] in the range of functional concentrations used in this work was examined with the MDCK cell lines (ESI†). The results revealed that up to 1 mM of CB[7] did not cause cell mortality. Thus 300 ng mL<sup>-1</sup> (0.86 nM) of C6 in the absence and in the presence of CB[7] (0.80 mM) were incubated with MDCK cell lines at 37 °C for 5, 15, 30, and 60 min. The large excess of CB[7] was added to ensure that the majority (>60%) of the C6 species was in the bound form. The CB[7]-assisted intracellular delivery of C6 was monitored *via* fluorescence microscopy. As shown in Fig. 3, incubation MDCK cells with C6@CB[7] complex resulted in inclusion of green fluorescent C6 within the cells, and the drug was likely located in the membrane and endosome without obvious accumulation in the nucleus. Interestingly, the fluorescence intensity within the cells gradually decreased from 5 min to 60 min, which is likely attributed to the initial CB[7] assisted C6 uptake in the complex form and subsequent release of free C6 in the cytoplasm (the fluorescence intensity of free C6 is much weaker in comparison with that of the CB[7]-complexed form,<sup>29</sup> as was seen from Fig. S1†). Detailed C6 distribution study by confocal laser scanning microscopy (ESI† Fig. S3 and a video showing z axis changes) confirmed that the C6 was mainly in the cytoplasm of the cells. In contrast, free C6 (either solubilized by Tween-80 or C6 suspension) exhibited little uptake by the MDCK cells regardless of incubation time. After the incubation treatment, the cells were rinsed three times with cold PBS and sonicated and ultra-centrifuged (13 000 rpm for 30 min) before the obtained supernatant was measured *via* fluorescence spectrophotometry. Interestingly the fluorescence emission resembled that of free C6, implying that C6 was released in the free form upon uptake by the MDCK cells. The C6 uptake therefore was quantitatively measured against its standard emission curve. The displacement of the included drug from CB[7] inside the cell environment is often desired for the purpose of

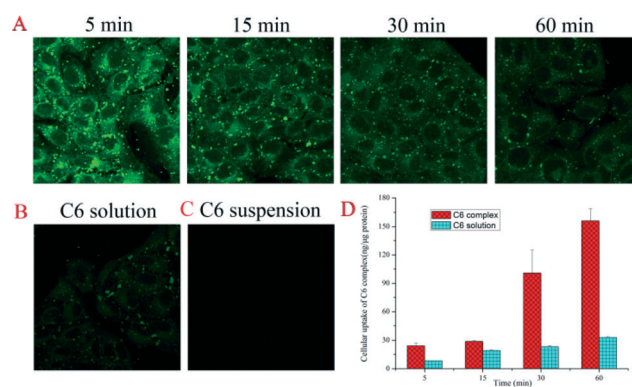


Fig. 3 Confocal laser scanning microscopy images of MDCK cell lines incubated for 5, 15, 30 and 60 min with C6@CB[7] (A), 60 min with C6 solution (solubilized by Tween-80) (B), and 60 min with C6 suspension (C6 suspended in HBSS) (C). And the quantitative cellular uptake of C6 by MDCK in the presence of CB[7] and Tween-80 (D) ( $n = 3$ ).



intracellular drug delivery, and presumably this process occurs *via* competitive guest binding by protein residues (amino acids).<sup>30</sup> Fig. 3D shows the performance of CB[7]-assisted cellular uptake of C6 quantitatively post incubation for different time-lengths. The cellular uptake increased gradually and reached a maximum at ~1 h. In the absence of CB[7], no detectable C6 was uptaken by the cells. Tween-80 was therefore added to enhance the solubility of C6 and facilitate free C6 intracellular transportation process,<sup>31</sup> for the sake of comparison. It seems that Tween-80 only moderately improved the cellular uptake of C6, which was still significantly less than the CB[7]-assisted uptake. The significant benefit of CB[7] in the intracellular uptake of a hydrophobic model drug is clearly demonstrated quantitatively here for the first time.

In order to understand the cellular uptake mechanism and investigate how a CB[7]-complexed hydrophobic drug would transport through an epithelial cell layer, endocytosis and exocytosis pathways were examined with several well-known and commonly used transcellular regulators (Table S1 in ESI† lists various inhibitors and the concentrations used in the study). For the endocytosis pathway detection, each of the regulators at a given concentration was pre-incubated with MDCK cells that were seeded in 12-well plates for 30 min. After the aspiration of the pre-incubated solutions, the C6@CB[7] complex (at the final concentrations of 0.86 nM C6 and 0.80 mM CB[7]) in HBSS and different inhibitors were added individually and further incubated at 37 °C for 30 min. This test was aborted by aspirating the dispersions and rinsing cells three times with cold PBS. The cells were subsequently scraped, washed and centrifuged according to the method described in the ESI† before the supernatant sample was measured by fluorescence spectrophotometry. For the exocytosis pathway study, the MDCK cell monolayer was incubated in a similar manner with the same concentration of the C6@CB[7] complex at 37 °C for 30 min first, and then inhibitors that were dissolved in HBSS (listed in Table S1†) were individually added to re-incubate the samples with cells for another 30 min at 37 °C during exocytosis process. The intracellular fluorescent intensities of C6 were measured *via* fluorescence spectrophotometry. As shown by Fig. 4, filipin, nystatin, EIPA and MβCD exhibited pronounced effects on the cellular uptake of the complex during the endocytosis and exocytosis processes, thus implying that the endocytosis and exocytosis of the complex involved clathrin and lipid raft-mediation, as well as macropinocytosis during this process. Conversely, the brefeldinA and Monensin exhibited no effect during the transportation of the C6@CB[7] complex, thus suggesting that ER/Golgi and Golgi/PM pathways were not involved.

The study was further extended to a larval zebrafish model to examine CB[7]-assisted *in vivo* uptake of the hydrophobic model drug. In recent years, zebrafish have emerged as useful vertebrate models for *in vivo* drug delivery including bio-availability and bio-distribution studies, due to the transparency of the whole body that enables non-invasive and direct

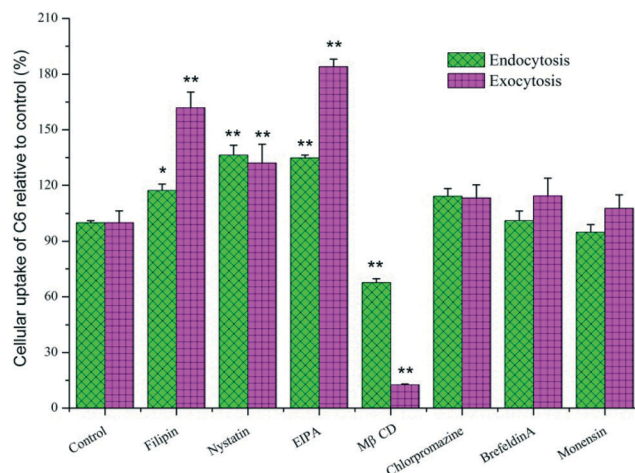


Fig. 4 Cellular uptake of C6 in the presence of CB[7] with various endocytosis/exocytosis regulators, as determined using ANOVA analysis in comparison with the control group (\* $p < 0.05$ , \*\* $p < 0.005$ ,  $n = 3$ ).

observations, especially by optical tracking of fluorescent probes.<sup>32,33</sup> Wild-type AB strain larval zebrafish at 8 days post fertilization were used for this study, as the structure and function of barrier and organs are similar to those of mammals.<sup>34</sup> The zebrafish (30/group) were incubated with the C6@CB[7] complex with concentrations of 100, 200, 400 and 800 ng mL<sup>-1</sup> of C6 with a large excess of CB[7] (930 equivalents by molecular ratio) for 30 min, respectively. Alternatively, the same concentration (300 ng mL<sup>-1</sup>) of C6@CB[7] was incubated for different time-lengths with the zebrafish samples. Equal quantities of the C6 suspension was added in the control groups, and Tween-80 solubilized C60 was added in groups of zebrafish for comparative purposes (ethical approval, detailed fish care, breeding, experimental and imaging protocols, are provided in the ESI†).

As was the case with the *in vitro* results, no obvious fluorescence was observed in larval zebrafish treated with free C6 suspension, weak fluorescence was observed in the Tween-80 solubilized C6 (C6 solution) treated groups, whereas strong fluorescence was observed in the C6@CB[7] complex treated groups (Fig. 5). In addition, when all groups of fish were treated with the same concentration of C6@CB[7] complex, the fluorescence emission intensity increased significantly when the duration of the incubation was increased from 5 to 30 min, and only increased moderately when the incubation time was increased from 30 to 60 min, indicating an *in vivo* uptake likely reached its maximum between 30 and 60 min of incubation (Fig. 5B). Additionally, this time dependent uptake behavior was further confirmed by the uptake quantification results (Fig. 5D). Moreover, a dose dependent *in vivo* uptake of the C6@CB[7] complex was demonstrated as well (Fig. 5C). Higher concentrations of the C6@CB[7] complex resulted in enhanced fluorescence emission intensity within the treated fish body after 30 min of incubation, which is consistent with the quantitative uptake data shown in Fig. 5E. In contrast, free C6 was barely taken up by zebrafish





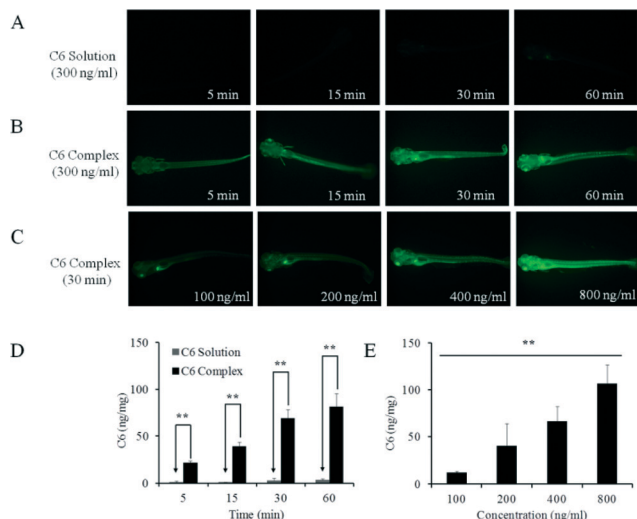


**Fig. 5** CB[7]-assisted C6 uptake in a larval zebrafish model. *In vivo* fluorescence images of zebrafish larvae treated with C6 solubilized by Tween 80 (0.2 wt%) at different time intervals (A), with C6 complex (300 ng ml<sup>-1</sup> C6 in the presence of 0.80 mM CB[7]) at different time intervals (B), and with C6 complex at various concentrations (C). Quantitative uptake of C6 by larval zebrafish at different time intervals (D), and different concentrations (E). Each data point is the mean of three determinations, with error bar representing the S.D. (*n* = 3) (\*\**p* < 0.01).

and the addition of Tween-80 only slightly enhanced the uptake.

It is interesting to note that when the C6@CB[7] concentration was at the lower range, the model drug preferentially targeted the eyes and the digestive system. Magnified fluorescent microscopic images of the zebrafish showed that the model drug preferentially accumulated in the following locations: the eyes, gall bladder, iridophores, and the microvascular system (Fig. S4 in ESI†). After uptake reached maximum, the extracted supernatant (in embryo medium) from the zebrafish exhibited a single fluorescence band with a maximum at 500 nm, which resembles the fluorescence spectrum of the free C6 solution. This result suggested once again that the free model drug C6 was eventually released from the C6@CB[7] species after it was taken up *in vivo* (likely in a cellular environment), which is often desired for a drug delivery system, where a lipophilic drug is transported into the targeted area and released at this site to impose its pharmacological activity.

In summary, we demonstrate for the first time the CB[7]-assisted quantitative *in vitro* and *in vivo* uptake of a hydrophobic model drug, by both an epithelial cell model (of a biological barrier) and a zebrafish model. The transcellular delivery pathway study suggested that multiple mechanisms were involved, including macropinocytosis, clathrin and lipid raft-mediated endocytosis/exocytosis. This study provides critical evidence to support the use of CB[7] as a carrier for lipophilic drugs in order to enhance their bioabsorption and bioavailability. The C6@CB[7] system may also find applications in both *in vitro* and *in vivo* environments as a chemosensor,

through competitive binding with other biologically important analytes.<sup>35,36</sup>

## Notes and references

- 1 R. K. Verma, D. M. Krishna and S. Garg, *J. Controlled Release*, 2002, **79**, 7–27.
- 2 S. Beg, S. Swain, M. Rizwan, M. Irfanuddin and D. S. Malini, *Curr. Drug Delivery*, 2011, **8**, 691–702.
- 3 T. Loftsson and M. E. Brewster, *J. Pharm. Pharmacol.*, 2010, **62**, 1607–1621.
- 4 D. S. Guo and Y. Liu, *Acc. Chem. Res.*, 2014, **47**, 1925–1934.
- 5 S. Walker, R. Oun, F. J. McInnes and N. J. Wheate, *Isr. J. Chem.*, 2011, **51**, 616–624.
- 6 D. H. Macartney, *Isr. J. Chem.*, 2011, **51**, 600–615.
- 7 M. E. Brewster and T. Loftsson, *Adv. Drug Delivery Rev.*, 2007, **59**, 645–666.
- 8 A. I. Rosenbaum, G. Zhang, J. D. Warren and F. R. Maxfield, *Proc. Natl. Acad. Sci. U. S. A.*, 2010, **107**, 5477–5482.
- 9 R. Lalor, H. Baillie-Johnson, C. Redshaw, S. E. Matthews and A. Mueller, *J. Am. Chem. Soc.*, 2008, **130**, 2892–2893.
- 10 A. I. Day and J. G. Collins, Cucurbituril Receptors and Drug Delivery, in *Supramolecular Chemistry: From Molecules to Nanomaterials*, ed. P. Gale and J. Steed, John Wiley & Sons, Ltd, 2012.
- 11 K. I. Assaf and W. M. Nau, *Chem. Soc. Rev.*, 2015, **44**, 394–418.
- 12 G. Hettiarachchi, D. Nguyen, J. Wu, D. Lucas, D. Ma, L. Isaacs and V. Briken, *PLoS One*, 2010, **5**, e10514.
- 13 V. D. Uzunova, C. Cullinane, K. Brix, W. M. Nau and A. I. Day, *Org. Biomol. Chem.*, 2010, **8**, 2037–2042.
- 14 R. Oun, R. S. Floriano, L. Isaacs, E. G. Rowan and N. J. Wheate, *Toxicol. Res.*, 2014, **3**, 447–455.
- 15 H. Chen, J. Y. W. Chan, X. Yang, I. W. Wyman, D. Bardelang, D. H. Macartney, S. M. Y. Lee and R. Wang, *RSC Adv.*, 2015, **5**, 30067–30074.
- 16 F. J. McInnes, N. G. Anthony, A. R. Kennedy and N. J. Wheate, *Org. Biomol. Chem.*, 2010, **8**, 765–773.
- 17 N. J. Wheate, V. Vora, N. G. Anthony and F. J. McInnes, *J. Inclusion Phenom. Macrocyclic Chem.*, 2010, **68**, 359–367.
- 18 N. J. Wheate, D. P. Buck, A. I. Day and J. G. Collins, *Dalton Trans.*, 2006, 451–458.
- 19 N. J. Wheate, *J. Inorg. Biochem.*, 2008, **102**, 2060–2066.
- 20 I. W. Wyman and D. H. Macartney, *Org. Biomol. Chem.*, 2010, **8**, 247–252.
- 21 R. Wang, D. Bardelang, M. Waite, K. A. Udachin, D. M. Leek, K. Yu, C. I. Ratcliffe and J. A. Ripmeester, *Org. Biomol. Chem.*, 2009, **7**, 2435–2439.
- 22 R. Wang and D. H. Macartney, *Org. Biomol. Chem.*, 2008, **6**, 1955–1960.
- 23 R. Wang, B. C. MacGillivray and D. H. Macartney, *Dalton Trans.*, 2009, 3584–3589.
- 24 P. Montes-Navajas, M. Gonzalez-Bejar, J. C. Scaiano and H. Garcia, *Photochem. Photobiol. Sci.*, 2009, **8**, 1743–1747.
- 25 G. Hettiarachchi, D. Nguyen, J. Wu, D. Lucas, D. Ma, L. Isaacs and V. Briken, *PLoS One*, 2010, **5**, e10514.



- 26 Z. Li, S. Sun, Z. Yang, S. Zhang, H. Zhang, M. Hu, J. Cao, J. Wang, F. Liu, F. Song, J. Fan and X. Peng, *Biomaterials*, 2013, **34**, 6473–6481.
- 27 S. S. Zhao, W. B. Dai, B. He, J. C. Wang, Z. G. He, X. Zhang and Q. Zhang, *J. Controlled Release*, 2012, **158**, 413–423.
- 28 C. Yu, B. He, M. H. Xiong, H. Zhang, L. Yuan, L. Ma, W. B. Dai, J. Wang, X. L. Wang, X. Q. Wang and Q. Zhang, *Biomaterials*, 2013, **34**, 6284–6298.
- 29 N. Barooah, J. Mohanty, H. Pal and A. C. Bhasikuttan, *J. Phys. Chem. B*, 2012, **116**, 3683–3689.
- 30 (a) M. A. Gamal-Eldin and D. H. Macartney, *Org. Biomol. Chem.*, 2013, **11**, 488–495; (b) J. W. Lee, H. H. L. Lee, Y. H. Ko, K. Kim and H. I. Kim, *J. Phys. Chem. B*, 2015, **119**, 4628–4636.
- 31 R. G. Strickley, *Pharm. Res.*, 2004, **21**, 201–230.
- 32 K. Jobe, C. H. Brennan, M. Motevalli, S. M. Goldup and M. Watkinson, *Chem. Commun.*, 2011, **47**, 6036–6038.
- 33 Y. Liu, Y. P. Wu, D. F. Feng, Q. J. Ye, X. Yang, X. Liu, C. Y. Gao, M. Wu, D. Y. Chen, Y. J. Zhang, L. Li and X. Z. Feng, *J. Mater. Chem.*, 2011, **21**, 18704–18710.
- 34 C. Chakraborty, C. H. Hsu, Z. H. Wen, C. S. Lin and G. Agoramoorthy, *Curr. Drug Metab.*, 2009, **10**, 116–124.
- 35 G. Ghale, A. G. Lanctot, H. T. Kreissl, M. H. Jacob, H. Weingart, M. Winterhalter and W. M. Nau, *Angew. Chem., Int. Ed.*, 2014, **53**, 2762–2765.
- 36 C. Kim, S. S. Agasti, Z. Zhu, L. Isaacs and V. M. Rotello, *Nat. Chem.*, 2010, **2**, 962–966.

